Photochemical & Photobiological Sciences

# Aspects of lanthanide complexes for the selectivity, strengthen and sharpness in luminescence bands from twenty-four praseodymium, europium and gadolinium complexes with differently distorted-hexadentate ligands



| | |
|---|---|
| Journal: | *Photochemical & Photobiological Sciences* |
| Manuscript ID | PP-ART-02-2020-000069.R1 |
| Article Type: | Paper |
| Date Submitted by the Author: | 19-Feb-2020 |





| | |
|---|---|
| Complete List of Authors: | Hasegawa, Miki; Aoyama Gakuin University<br>Sakurai, Shoya; Aoyama Gakuin University<br>Yamaguchi, Masafumi A.; Aoyama Gakuin University<br>Iwasawa, Daichi; Aoyama Gakuin University<br>Yajima, Naho; Aoyama Gakuin University<br>Ogata, Shuhei; Aoyama Gakuin University<br>Inazuka, Yudai; Aoyama Gakuin University<br>Ishii, Ayumi; JST/PRESTO<br>Suzuki, Kengo; Hamamatsu Photonics K. K. |

Journal Name

ARTICLE

# Aspects of lanthanide complexes for the selectivity, strengthen and sharpness in luminescence bands from twenty-four praseodymium, europium and gadolinium complexes with differently distorted-hexadentate ligands†

Received 00th January 20xx,
Accepted 00th January 20xx

DOI: 10.1039/x0xx00000x

www.rsc.org/

Miki Hasegawa*[a,b], Shoya Sakurai,[a] Masafumi Andrew Yamaguchi,[a] Daichi Iwasawa,[a] Naho Yajima,[a] Shuhei Ogata,[a] Yudai Inazuka,[a] Ayumi Ishii[b,c,d] and Kengo Suzuki[e]

We structually and spectroscopically investigated a series of praseodymium (Pr) complexes with eight ligands that form helicate molecular structures. The mother ligand skeleton (L) has two bipyridine moieties bridged with ethylenediamine. The bridged skeleton of PrL was changed to diamines 1-methyl-ethylenediamine, trimethylenediamine and 2,2'-dimethyl-trimethylenediamine, and the corresponding ligands were designed $L^{me}$, $L^{pr}$ and $L^{dmpr}$. Each Pr in these complexes upon UV-excitation. The luminescence quantum yields of PrL and $PrL^{pr}$ in the visible and near infrared (NIR) regions indicate that PrL is excited by both the electronic state of the ligand and the ff absorption band, whereas $PrL^{pr}$ is excited through the ligand. The addition of a methyl group to PrL and $PrL^{pr}$ has different effect on the Pr emission intensity with the intensity of $PrL^{me}$ decreasing more than that of PrL and $PrL^{dmpr}$ increasing more than that of $PrL^{pr}$. Thus, the coordination of Pr and the increased rigidity of the ligand pon methylation enhance luminescence. The azomethine moieties on $L^{me}$, $L^{pr}$ and $L^{dmpr}$ were reduced and formed the corresponding PrLH, $PrL^{me}H$, $PrL^{pr}H$ and $PrL^{dmpr}H$ complexes. The luminescence of the non-methylated series is due to transition related to the $^1D_2$ level and thus the methylated series luminesces due to high energy levels such as $^3P_J$ arising from the shortened π electronic systems. We also discuss the strong red emission of a series of Eu complexes with eight ligands from the viewpoint of their molecular structures and luminescence efficiencies and evaluate the Judd-Ofelt parameters from the luminescence spectra of Eu complexes.

## Introduction

Luminescent materials with trivalent lanthanide (Ln) ions are widely interested because of their stable luminescence colour assigned to the typical ff transitions localized on metal centres. For the design of molecular shape with luminescence properties in Ln complexes, it relatively depends on experiences base on phenomena or in literatures already reported due to the difficulty to expect the binding-direction of neighbor coordination atoms/ions or to no hybridized orbital theory. Finally the molecular design of luminescent Ln complexes needs unique points to induce the ability of photo-antenna effect based on the coordination between ligands[1] and Ln having the shortest distances, the energy levels-corresponding between the donor in excited ligands and accepter in Ln ion, and keeping the spin conservation law of spin multiplicities on the energy donor and accepter levels.[2, 3] The design of the molecules and energy states between the ligand and Ln ions were considered based on these approaches for the highly luminescent complex formations of Eu complexes.[4, 5] Also, coordination symmetry or ligand distortion will also enhance their luminescence ability through the antenna effects.[6,7]

The luminescence bands of trivalent praseodymium (Pr) appear in a wide wavelength region from the UV to near infrared (NIR), due to their split f levels which have a unique spin multiplicity. These luminescence bands arising from ff transitions are sensitized with the coordination of organic compounds which act as photo-antenna upon UV irradiation.[1,8] Inner relaxation events compete with luminescence intensity, resulting in a weaker intensity of ff emission of Pr compared to europium (Eu) ion due to the electronic structure of Pr. There some reports to provide the strategy of efficient luminescent Ln complexes even in solutions.[9,10] The luminescence behaviour of Pr provides information pertinent to its application in electric devices and in understanding the probability of energy transfer.

[a] Department of Chemistry and Biological Science, College of Science and Engineering, Aoyama Gakuin University, 5-10-1 Fuchinobe, Chuo-ku, Sagamihara, Kanagawa 252-5258 Japan. E-mail: hasemiki@chem.aoyama.ac.jp; Fax: +81-42-759-6221
[b] Mirai Molecular Materials Design Institute, Aoyama Gakuin University, 5-10-1 Fuchinobe, Chuo-ku, Sagamihara, Kanagawa 252-5258, Japan
[c] JST, PRESTO, 4-1-8 Honcho, Kawaguchi, Saitama 332-0012, Japan.
[d] Graduate School of Engineering, Toin University of Yokohama, Kurogane-cho, OAoba-ku, Yokohama, Kanagawa,225-8503, Japan
[e] Hamamatsu Photonics K. K., 812 Joko-cho, Higashi-ku, Hamamatsu, Shizuoka 341-3196, Japan

†Supplementary Information (ESI) available: Packing structures of Pr and Eu complexes, excitation spectra, NIR-luminescence spectra, luminescence decay profiles, calculation of energy transfer efficiencies, energy diagram of Pr-luminescencent complexes and $^1H$ NMR of each ligand. See DOI: 10.1039/x0xx00000x

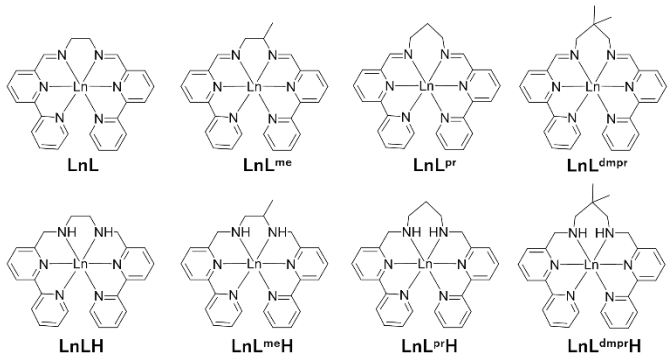


**Fig. 1** Designed molecular structure of a series of helicate complexes with Ln (Ln = Pr, Gd or Eu). Counter anions are omitted for clarity.

Emission enhancement of ff transitions of Pr ion is usually difficult because the electron configuration of the Pr ion causes internal conversion during energy relaxation process. Actually, only few Pr complexes were succeeded to intensify their luminescence in Metal-Organic-Frameworks with twitterionic-ligands or using four energy transfer pathways from $^1S_2$*, $^1S_1$* excited ILCT(intra-ligand charge transfer) and $^3$T* states.[11,12]

The number of scientific papers examining the utility of Pr complexes in electrical engineering and bio-stimuli luminescence has increased over the past decade.[13,14] For instance, the addition of Pr ion to ceramics such as GaN and $(Bi_{0.5}Na_{0.5})TiO_3$ induces red emission due to defects in the crystal structure.[15, 16] Mixed metal complex systems with Pr and Dy were reported as a white-light emission material.[17] Such characteristic electronic transitions have been the focus of several investigations, such as that of the absorption and luminescence spectra of Pr complexes with selected phosphonate ligands.[18,19]

The ff absorption bands of a series of Pr complexes and their red or NIR luminescence characteristics by UV excitation have been examined.[20-34] For instance, ternary Pr complexes with dithiocarbamate with 1,10-phenanthroline or 2,2'-bipyridine were examined their photoluminescence properties because the intensities were notably high.[29] In addition, d-f multinuclear complexes have been synthesized and their up-conversion properties and the sensitization of ff emissions by the metal-to ligand charge transfer transition states.[35,36] Energy transfer pathway of Pr complexes was examined with the comparison of the excited state as energy donor of aromatic compounds (EnD) and split-f levels of Pr ion as an accepter (EnA).[27, 37, 38] We previously reported the selective luminescence of Pr complexes with a series of phenanthroline ligands based on the picosecond time-resolved luminescence spectra.[39] The split f-levels of a trivalent Pr ion adopt both singlet and triplet states and ligand elongation/shortening clearly affects the Dexter type-energy transfer pathway. Thus, it indicates the need to understand the principle of energy transfer in Pr complexes by using spin multiplicities fitting the transition energies between the ligand as EnD and Pr as EnA.

Here, we report a series of helicate Ln complexes with eight organic ligands (Fig. 1). Helicate and high-chelate effective complexes with Ln were reported for a structural interesting and stability in solutions.[40,41] The mother ligand, L, has two bipyridine moieties bridged with ethylenediamine and forms stable structured monodentate complexes with a series of lanthanide ions.[42-46] The Eu complex, EuL, shows a high luminescence quantum yield (QY) of over 55% in the solid state and a QY of 12% in acetonitrile. These high QY values are caused by the efficiency of the energy donor level located in the excited triplet state of L for forwarded intramolecular energy transfer. The energy donor level of trivalent Pr ion is similar to that in Eu ion. The spin states of Pr ion are unique because the split f-orbitals have singlet and triplet states, as well as the major multiplicities of organic compounds.[47-50] We previously reported the energy transfer from the excited triplet state of the ligand of Pr complexes with phenanthroline derivatives (Pr-phen) to the triplet accepter level of the Pr ion, [38] and that such energy transfer does not occur in the singlet state due to the Dexter mechanism.[51] Pr also luminesces in NIR region, and some literatures show enhancement of the NIR luminescence in Pr complexes.[21, 24, 33, 34]

The selective energy transfer properties of Pr complexes led us to design a series of lanthanide complexes. We examined the structures of PrL, PrLme, PrLpr, PrLdmpr, EuLme, EuLpr and EuLdmpr, and electronic transitions of twenty four-complexes by single X-ray structural analyses and their electronic spectra. Eu complexes with the ligands were also characterized to shed light on the energy transfer properties of these ligand complexed with Pr ion.

## Results and discussion

### Structural analyses of Pr and Eu complexes with L, $L^{me}$, $L^{pr}$ and $L^{dmpr}$.

Compound L is a hexadentate ligand that wraps around a Pr ion in which two nitrate oxygen atoms coordinate to the metal. A series of Pr complexes with L and its derivatives were synthesized, single crystals prepared, and the structures analyzed, as shown in Fig. 2 and Table S1. Three Eu complexes, with $L^{me}$, $L^{pr}$ and $L^{dmpr}$, are also shown in the figure. PrL and $PrL^{me}$ an isoform of other previously reported Ln complexes.[42, 43, 46] The interatomic distances between the Pr ion and the coordinating atoms in PrL are also belong the trend in the lanthanide contraction with those of LnL complexes.

$PrL^{me}$ was crystallized as a racemic mixture of *R*- and *S*-type bridging sites in the complex. The complex forms a helicate structure, with two nitrate ions at the apical sites. The dihedral angles of the two bpy moieties in $PrL^{me}$ were larger than that in PrL. $PrL^{pr}$ and $PrL^{dmpr}$ also adopted helicate structures, and the dihedral angel between the two bpy moieties in $PrL^{pr}$ was larger than those of the other three complexes.

We obtained single crystals of $EuL^{pr}$ and $Eu^{dmpr}$. As shown in Fig. 2, the molecular formation of each Eu complex is that of the Pr complex with the corresponding ligand, indicating that each Eu complex forms helicate structures with different degrees of distortion (Table S2). Very recently, we found circularly

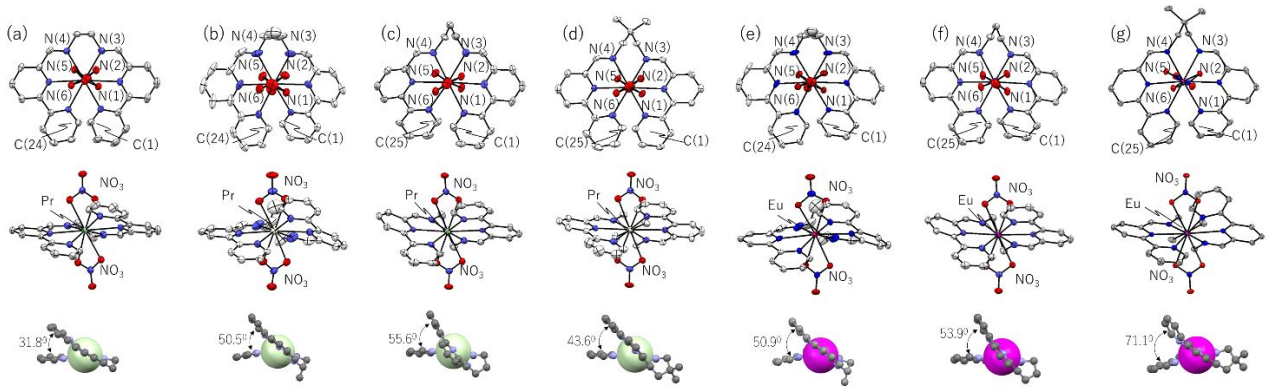


dichroism localized on the ligand and circularly polarized luminescence of centre metal ion in EuL$^{me}$ in acetonitrile.[45]

**Fig. 2** Top and middle: ORTEP drawings of four praseodymium complexes and three europium ones, (a) PrL, (b)PrL$^{me}$, (c) PrL$^{pr}$, (d) PrL$^{dmpr}$, (e) EuL$^{me}$, (f) EuL$^{pr}$ and (g) EuL$^{dmpr}$. Hydrogen atoms, $PF_6^-$ and acetonitrile are omitted for clarity. Bottom: their side views to compare the dihedral angles among two bipyridine moieties. Grey: carbon, blue: nitrogen, red: oxygen, pale green: praseodymium, and pink: europium. For each of the illustration, $NO_3^-$ ions are omitted for clarity. EuL$^{me}$ was published in ref 46.

From the measurement of single crystal X-ray analysis of a racemic crystal of EuL$^{me}$, this complex keeps the helicate structure as shown in Figure 2 for comparison. Space groups in Pr complexes with the four ligands differ (Table S1), and correspond to those in Eu complexes with L[41], L$^{me}$ [46]and L$^{pr}$. The molecular packing of PrL is similar to that of EuL.[41]

The structural comparison between EuL and EuLH were already reported from the measurements of single crystal X-ray analyses.[56] For example, dihedral angles of EuL was 32.0$^{O}$.[42] EuLH takes two takes two molecular systems in the unit cell, and the dihedral angles were 61.7$^{O}$ and 48.8$^{O}$. We also tried to recrystallize other complexes especially with a series of reduced ligand, but the crystal qualities of them were not enough for X-ray analyses. The relation of the structural aspects and spectral behaviour will explain later.

**Substitution on the helicate Eu complexes and their luminescence behaviour.**

Much fundamental information is available regarding the nature of electronic transitions of Eu complexes.[52, 53] EuL was already reported[42] as an initial complex for the present series of complexes and the Eu ion luminesces in the red-wavelength region. The QY of EuL in the solid state was over 50% and it retains its luminescence in acetonitrile (QY =12%) and ionic liquids (32.3%)[45] because of the molecular stability conferred by the chelate effect with hexadentate ligands. We previously reported the single ionic magnetic properties of dysprosium and neodymium complexes with L.[43] The electronic structures of these complexes with L are retained even in the solid state with decreased intermolecular interactions.

Fig. 3, S2 and S3 show luminescence, excitation spectra and decay profiles, respectively, of EuL$^{me}$, EuL$^{pr}$ and EuL$^{dmpr}$ in the solid state and in acetonitrile, together with the corresponding data of EuL[42] and EuL$^{me}$[46]. Each complex shows typical luminescence of Eu ion in the wavelength region 580-740 nm. The band around 590 nm is split into two or three in them. For instance, EuL shows two split bands at 590.3 and 597.6 nm in the solid state, and 590.0 and 595. 8nm in acetonitrile, which

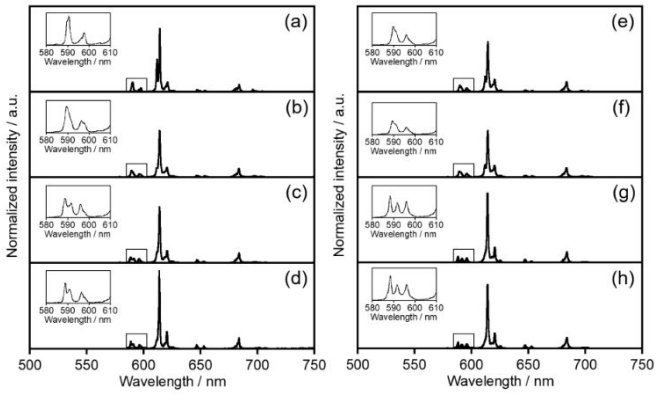


**Fig. 3** Luminescence spectra of (a, e) EuL[42], (b, f) EuL$^{me}$[46], (c, g) EuL$^{pr}$, and (d, h) EuL$^{dmpr}$ in the solid (left column) and in acetonitrile (right column). Inset shows the $^5D_0 \rightarrow {}^7F_1$ band. $\lambda_{ex}$ =300 nm.

can be assigned to the $^5D_0 \rightarrow {}^7F_1$ transition. These band positions similarly appeared for EuL$^{me}$. While EuL$^{pr}$ shows corresponding bands at 588.7 and 596.1 with new 591.7 nm band in the solid and at 588.3 and 596.0 nm with 591.5 nm in acetonitrile. The newly appeared bands can be attributed to the $^5D_1 \rightarrow {}^7F_3$ transition of Eu ion.[54, 55] The band appearance was also recognized in EuL$^{dmpr}$ in both states. From the structural analyses of Ln complexes with a series of L, we can categorize the coordination shapes of ligand moieties, especially, the pentagon and hexagon formation in the centre chelate ring after the coordination. For example, L and L$^{me}$ have former chelate ring and L$^{pr}$ and L$^{dmpr}$ do latter. Thus, the appearance of the $^5D_1 \rightarrow {}^7F_3$ transition suggest the distorted coordination sphere.

The luminescence lifetimes, QY and calculated photophysical data (ESI) are summarized in Table 2 and Fig. S4. The observed QY ($\varphi_{obs}$) of EuL$^{pr}$ in the solid state is almost the same as that of EuL, whereas the QY values of EuL$^{me}$ and Eu$^{dmpr}$ are lower and higher than EuL and EuL$^{pr}$, respectively. This trend for Eu complexes in acetonitrile corresponds to that for Pr complexes

**Table 2** Photophysical data of luminescence for EuL[42], EuL$^{me}$ [46], EuL$^{pr}$, EuL$^{dmpr}$ in the solid and in acetonitrile. $\Omega_2$, $A_{rad}$, $A_{nr}$, $\tau_{rad}$, $\varphi_{Ln}$, $\varphi_{obs}$ and $\eta_{EnT}$ are Judd-Ofelt parameter, radiative rate constant ($s^{-1}$), non-radiative rate constant ($s^{-1}$), luminescence lifetime (ms), metal-centred luminescence efficiency, observed quantum yield by ligand excitation and energy transfer efficiency, respectively.

| | in the solid state | | | | in acetonitrile | | | |
|---|---|---|---|---|---|---|---|---|
| | EuL | EuL$^{me}$ | EuL$^{Pr}$ | EuL$^{dmpr}$ | EuL | EuL$^{me}$ | EuL$^{Pr}$ | EuL$^{dmpr}$ |
| $\Omega_2$ x$10^{-20}$ | 8.42 | 7.46 | 7.74 | 8.56 | 7.88 | 7.59 | 8.95 | 7.51 |
| $A_{rad}$ | 369.6 | 532.0 | 352.0 | 371.5 | 261.2 | 255.2 | 283.4 | 255.0 |
| $A_{nr}$ | 499.9 | 600.4 | 548.3 | 521.4 | 384.0 | 520.0 | 425.8 | 429.9 |
| $\tau_{rad}$ | 1.15 | 1.05 | 1.11 | 1.12 | 1.55 | 1.29 | 1.41 | 1.46 |
| $\varphi_{Ln}$ | 42.5 | 37 | 39.1 | 41.6 | 40.5 | 32.9 | 40 | 37.2 |
| $\varphi_{obs}$ | 52.6% | 34.3% | 51.1% | 64.6% | 12% | 17.5% | 9.6% | 28% |
| $\eta_{EnT}$ | >99% | 92.8% | >99% | >99% | 22.6% | 53.2% | 24% | 75.2% |

**Table 3** Luminescence lifetimes (Amplitude) and QY of EuLH[56,57], EuL$^{me}$H, EuL$^{pr}$H and EuL$^{dmpr}$H in the solid state and in acetonitrile. $\tau_{rad}$ ($s^{-1}$) and $\varphi_{obs}$ are luminescence lifetime (ms) and observed quantum yield, respectively.

| | in the solid state | | | |
|---|---|---|---|---|
| | EuLH | EuL$^{me}$H | EuL$^{Pr}$H | EuL$^{dmpr}$H |
| $\tau_{rad}$ | 0.48 (0.70), 0.22 (0.30) | 0.26 (0.81), 0.14 (0.19) | 0.43 (0.65), 0.13 (0.35) | 0.51 (0.66), 0.30 (0.34) |
| $\varphi_{obs}$ | 12.6% | 7.3% | 9.5% | 13.3% |
| | in acetonitrile | | | |
| | EuLH | EuL$^{me}$H | EuL$^{Pr}$H | EuL$^{dmpr}$H |
| $\tau_{rad}$ | 0.27 (1.00) | 0.25 (0.66), 0.42 (0.34) | 0.32 (0.91). 1.12 (0.09) | 0.43 (0.62), 0.66 (0.38) |
| $\varphi_{obs}$ | 5.3% | 5.8% | 8.9% | 14.9% |

as described later, suggesting that methylation acts as a deterrent to reduce structural vibration in the electronic transition as described later.

The Judd-Ofelt parameter ($\Omega_2$) for evaluating the effect of deterrent to reduce structural vibration in the electronic transition as described later.

The Judd-Ofelt parameter ($\Omega_2$) for evaluating the effect of symmetry around the Eu ion was estimated from the observed physicochemical values (ESI). For instance, the $\Omega_2$ value of EuL in acetonitrile was 7.88x$10^{-20}$, which is rather large, possibly indicating EuL has low symmetry. The $A_{nr}$ value of EuL in solution was also low. Together, these results suggest a high QY, but in fact QY was only 12%, possibly due to vibrational dampening by the medium, as is not so high. It was caused by the deactivation with the vibration of medium, as supported by the low value of $\eta_{EnT}$.

The luminescence spectra of EuLH,[56, 57] EuL$^{me}$H, EuL$^{pr}$H and EuL$^{dmpr}$H in the solid state and in acetonitrile are shown in Fig. S5. The position of each band in the solid state corresponds to that in acetonitrile. The luminescence lifetimes and QY of these complexes are summarized in Table 3. It is noteworthy that the observed $^5D_0$-$^7F_1$ transitions in EuL, EuL$^{me}$, EuLH and EuL$^{me}$H in acetonitrile were split into two and into three in EuL$^{pr}$, EuL$^{dmpr}$, EuL$^{pr}$H and EuL$^{dmpr}$H. As described above, the middle band between the two-split $^5D_0$-$^7F_1$ transition of Eu is assigned to the $^5D_1$-$^7F_3$ transition. The $^5D_1$-$^7F_3$ band means the high distortion around Eu ion. Actually, after the reduction of azomethine moieties in a series of L, the single C-N bonds in LHs will enhance the higher distortion than the double C=N bonds, even during the energy relaxation processes.[44] Actually, the bridgingethylendiaimne site of EuLH is more flexible than that of EuL.[56] The luminescence lifetimes of the ff transition band ina series of LHs show at least two components both in the solid and acetonitrile.

Previously we reported the reduced effect of azometine moiety on their luminescence property.[55] For example, luminescence quantum yields of EuLH and EuL were 5.3% and 12.0%, respectively. It was caused by the differences between energy donor and acceptor levels. The energy differences in EuLH is higher than that in EuL due to the shortened π-electronic systems of the ligand. Similarly, the luminescence quantum yields of LH-derivatives of become lower than those of L-derivatives.

In the solid state, it looks no enhancement of helicity on the luminescence properties in both derivatives of EuL or that of EuLH. While in acetonitrile, their methylation of bridging site, ethylenediamine or trimethyelendiamine affect to the increasing in luminescence quantum yields, owing to the high $k_{nr}$ by the prohibition of intramolecular fluctuation. In acetonitrile. Thus, it found that the energy donor ability takes precedence over the helicity in these Eu complexes.

**Selective luminescence of Pr complexes with L, L$^{me}$, L$^{pr}$ and L$^{dmpr}$ and comparison of their excited triplet state in Gd complexes.**

The luminescence and excitation spectra of PrL, PrL$^{me}$, PrL$^{pr}$ and PrL$^{dmpr}$ in the solid state and in acetonitrile, together with Gd complexes with corresponding ligand are shown in Fig. 6 and S6. The use of fluorescence and phosphorescence localized on the ligand of the Gd complex provides information on the energy donor properties of the ligands of lanthanide complexes.[58] The fluorescence and phosphorescence band positions are summarized in Table S3.

PrL in acetonitrile show luminescence bands 489, 531, 546, 602, 610, 632, 651661, 683, 706, 1025 and 1045 (sh) nm, and were assigned to the $^1I_6$→$^3H_4$, $^3P_1$→$^3H_4$, $^3P_1$→$^3H_5$, $^3P_0$→$^3H_5$, $^1D_2$→$^3H_4$, $^3P_0$→$^3H_6$, $^3P_1$→$^3F_2$, $^3P_0$→$^3F_2$, $^3P_0$→$^3F_3$, $^1D_2$→$^3H_5$, $^1D_2$→$^3F_3$ and $^1D_2$→$^3F_4$ transition (Fig. S7), respectively. These bands appear at similar positions in the solid state.

The other three Pr complexes in acetonitrile show corresponding bands at similar positions and of similar intensity but differed for each other. The most intense band appeared around 610 nm in both the solid state and acetonitrile, whereas othe NIR luminescence intensity of PrL in the solid state is very weak. The NIR emission of Pr in the solid state was stronger than that in PrL$^{me}$ and PrL$^{dmpr}$, but not in PrL$^{pr}$. A previous theoretical study of TbL[44] showed that the bridged moiety of the ligand is distorted in the excited state during the energy relaxation process resulting to a large effect on non-radiative relaxation. Thus, the methylation of ethylene-diamine or trimethylene-diamine maintains the stiff skeleton in the excited state, and thus the non-radiative relaxation in methylation derivatives of

PrL will be lower than those of PrL derivatives without methyl groups.

The triplet state of $L^{me}$ and $L^{pr}$ of Gd complexes in solutions were more blue-shifted than in the solid states (Table S3), whereas Gd complexes with L and $L^{dmpr}$ in solution showed no shifts compared to that in the solid state. Molecular distortion in the helicate ligand accelerates the emission from higher energy levels in Ln ions. The spectral differences between the four Pr complexes correspond to the trend in dihedral angles between the two π electronic systems as shown in Fig. 2.

Four other Pr helicate complexes with the shortened π electronic systems (LH, $L^{me}H$, $L^{pr}H$ and $L^{dmpr}H$) were generated by the reduction of L, $L^{me}$, $L^{pr}$ and $L^{dmpr}$ and their luminescence spectra were observed. The π-electronic transitions of the corresponding Gd complex are also shown. The ff luminescence bands of PrLH appear at the same position in PrL. The phosphorescence band of GdLH appeared at shorter wavelength regions of GdL, indicating that the energy donor level of the ligand of PrLH is higher than in PrL.[39] $PrL^{me}H$, $PrL^{pr}H$ and $PrL^{dmpr}H$ showed similar spectral changes as $PrL^{me}$, $PrL^{pr}$ and $PrL^{dmpr}$(Figs. 4, 5 and Table S3). The phosphorescence bands of Gd complexes with the same role as the energy donor of PrLH, $PrL^{me}H$, $PrL^{pr}H$ and $PrL^{dmpr}H$ were higher than those of PrL, $PrL^{me}$, $PrL^{pr}$ and $PrL^{dmpr}$ in both solution and solid state.

Finally, the luminescence of these eight Pr compelxes indicates to categorize that selectivity of ff emissions of Pr in this series depend on the reduction/non-reduction of azomethine moiety because of their different energy donor levels (Fig. 6). Also, the ligand distortion makes to intense the ff emission of Pr ions even in solution.

From the consideration of Dieke's diagram, the band position of acceptor level of Pr which luminesces in NIR region superimposes the luminescence band position of own VIS-luminescence. For the measurements of NIR luminescence QY in PrL, $Pr^{me}$, $PrL^{pr}$ and $PrL^{dmpr}$, we used both excitation wavelengths corresponding to the bands of ligand and ff-absorption band. Here, we focus on the results of PrL and $PrL^{pr}$. Then, the NIR-luminescence QY value of PrL excited by the ff-absorption band is higher than that by the ligand, indicating that the NIR luminescence is able to be sensitized by the ligand and ff-absorption-band excitation in PrL (Fig. S8 and Table S4). While, the NIR-luminescence QY value of $PrL^{pr}$ excited by ff-absorption-band is as well as that by ligand excitation, meaning that both emissions were induced by the antenna effect. Thus, molecular distortion will affect the energy transfer pathway in Pr complexes. We believe it is the first aspect to concern the dual excitation ability of Pr complexes with molecular distortion result in the NIR luminescence. The trend of the QY values for the order of these Pr complexes show similarity in those of Eu complexes.

The relation between the QY values of Eu complexes and the molecular distortion as dihedral angles of two bpy moieties is along the distortion. The helicate degree is defined as the dihedral angle between the bpy moieties, which resulting in the order of LnL, $LnL^{me}$, $Ln^{pr}$ and $LnL^{dmpr}$. It indicates the luminescence ability surely depends on the π-electronic distortions. This result is suitable compared with previous

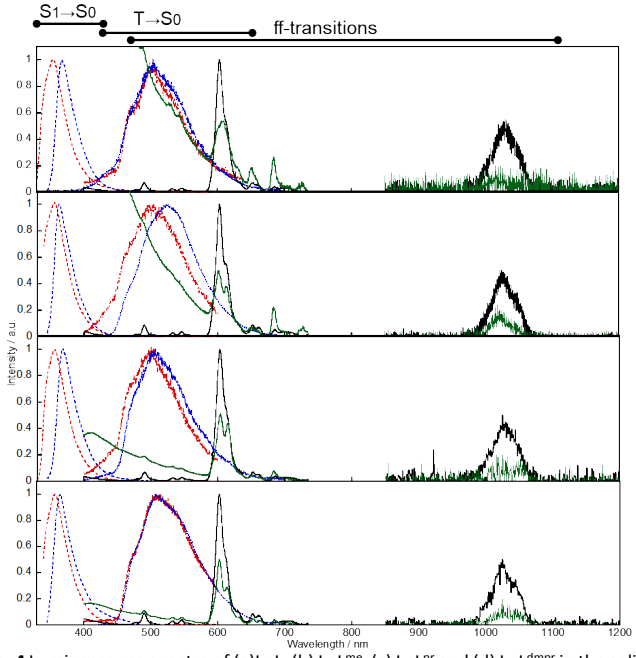


**Fig. 4** Luminescence spectra of (a)LnL, (b) $LnL^{me}$, (c) $LnL^{pr}$ and (d) $LnL^{dmpr}$ in the solid state (green for ff- and blue for ππ transitions; Ln=Pr) and in acetonitrile (black for ff- and red for ππ transitions; Ln=Gd). The ππ transitions localized on the ligands in a series of Gd complexes were observed at 77 K. $\lambda_{ex}$= 300 nm.

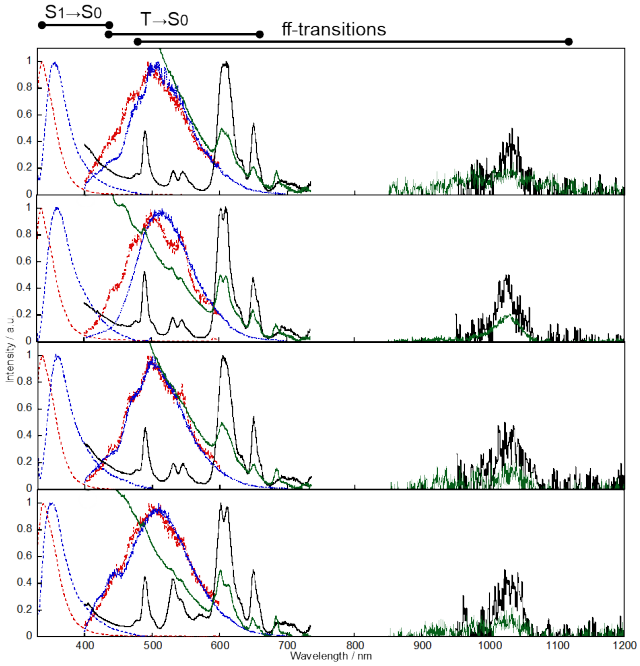


**Fig. 5** Luminescence spectra of (a) LnLH, (b) $LnL^{me}H$, (c) $LnL^{pr}H$, and (d) $LnL^{dmpr}H$, in the solid state (green for ff- and blue for ππ transitions; Ln=Pr) and in acetonitrile (black for ff- and red for ππ transitions; Ln=Gd). The ππ transitions bands localized on the ligands in a series of Gd complexes were observed at 77 K. $\lambda_{ex}$= 300 nm.

reports.[44] Whereas in the case of Pr complexes, although the quantum yield of $PrL^{dmpr}$ was the highest, the values were not in the order of molecular distortions. Thus, methylation of the bridging site on the ligand maintains the rigidity of the molecule even in the excited state, consistent with the increased intensity of ff emission in case of the tripheylene moiety. We will consider the molecular distortion with the effective methylation in the

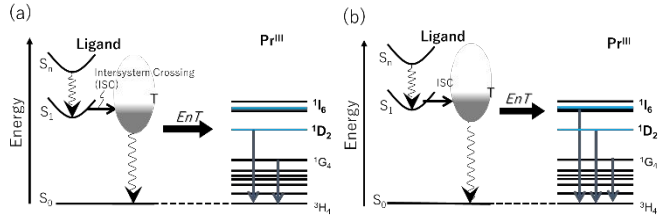


**Fig. 6** Energy relaxation diagrams of ff emission in a series of (a) PrL and of (b) PrLH. Notation of $^3P_J$ states around $^1I_6$ are omitted for clarity.

antenna ligand for getting the high luminescence lanthanide compounds.

## Experimental

### Synthesis of hexadentate ligands

The initial hexadentate ligands, L and LH, were prepared as described previously.[42, 59] Three hexadentate ligands, $L^{me}$, $L^{pr}$ and $L^{dmpr}$, were synthesized by the reaction of 2 eq. of bipyridine-6-aledehyde (CHO-bpy) and 1 eq bridging amine (either propane-1,2-diamine, propane-1,3-diamine or 2,2-dimethylpropane-1,3-diamine, respectively). The reduced compounds, $L^{me}H$, $L^{pr}H$ and $L^{dmpr}H$, were synthesized by the same method as used to obtain LH. Characterization were summarized in ESI (Fig. S9).

**$L^{me}$.** CHO-bpy (100 mg; 0.543 mmol) in 5 ml methanol was stirred with 19.0 mg of propane-1,2-diamine (0.256 mmol) for 3 h, and a yellowish oil was obtained as $L^{me}$ after vacuum drying. Yield: 96.4 mg (0.238 mmol, 92.8 %), $^1$H-NMR (500 MHz, $CDCl_3$); $\delta$ 8.69 ppm (2H, d), 8.54 (1H, s), 8.50 (1H, s), 8.45 (2H, d), 8.40 (2H, d), 8.37 (2H, d), 8.08 (2H, d), 8.03 (2H, d), 7.84 (2H, t), 7.78 (2H, t), 7.29 (2H, d), 3.95 (2H, m), 3.43 (1H, s), 1.43 (3H, d).

**$L^{pr}$.** CHO-bpy (100 mg; 0.543 mmol) in 5 ml methanol was stirred with 20.5 mg of 1,3-propanediamine (0.277 mmol) for 3h. $L^{pr}$ was obtained as a yellowish oil after vacuum drying. Yield: 105 mg (0.259 mmol 93.4 %), $^1$H-NMR (500 MHz, $CDCl_3$); $\delta$ 8.67 ppm (2H, d), 8.54 (2H, s), 8.45 (2H, d), 8.40 (2H, d), 8.06 (2H, d), 7.88 (2H, t), 7.80 (2H, t), 7.31 (2H, t), 3.86 (4H, t) and 2.23 (2H, m) ppm. $PrL^{pr}$ was prepared using 100 mg $L^{Pr}$ and 111.8 mg $Pr(NO_3)_3 \cdot 6H_2O$ in ethanol. Yield 176 mg (0.240 mmol, 97.2 %). MS (FAB+); m/z, 671.09 [M – $NO_3^-$]+ (calcd. 671.07). These complexes were crystalized from a mixed solution of acetonitrile and diethylether.

**$L^{dmpr}$.** CHO-bpy (100 mg; 0.543 mmol) in 5ml methanol was stirred with 27.5 mg (0.269 mmol) of 2,2-dimethyl-1,3-propanediamine for 3 h. The obtained yellowish oil was characterized as $L^{dmpr}$. Yield: 118 mg (0.272 mmol, >99%), $^1$H-NMR (500 MHz, $CDCl_3$); $\delta$ 8.68 ppm (2H, d), 8.51 (2H, s), 8.44 (4H, m), 8.12 (2H, d), 7.86 (2H, t), 7.78 (2H, t), 7.29 (2H, d), 3.67 (4H, s), 1.12 (6H, s).

**$L^{me}H$.** As-obtained $L^{me}$ in methanol was reduced by the adding 0.05 g (1.32 mmol) of $NaBH_4$ for 1 h, and $L^{me}L$ was obtained as a yellowish oil. Yield: 86.9 mg (0.212 mmol, 78 %), $^1$H-NMR (500 MHz, $CDCl_3$); $\delta$ 8.64 ppm (2H, d), 8.39 (2H, d), 8.24 (2H, d), 7.72 (4H, d+t), 7.29 (4H, dt), 4.08 (1H, m), 3.95 (2H, d), 2.74 (4H, dd), 1.18 (3H, d).

**$L^{pr}H$.** The ligand was synthesized using the same method as for $L^{me}H$. Yield: 90.8 mg (0.221 mmol, 81.5 %), $^1$H-NMR (500 MHz, $CDCl_3$); $\delta$ 8.66 (2H, d), 8.40 (2H, d), 8.24 (2H, d), 7.74 (4H, m), 7.27 (4H, m), 3.98 (4H, s), 2.82 (4H, m), 1.86 (2H, m).

**$L^{dmpr}H$.** The ligand was synthesized using the same method as for $L^{me}H$. Yield: 90.8 mg (0.207 mmol, 76.3%), $^1$H-NMR (500 MHz, $CDCl_3$); $\delta$ 8.65 ppm (2H, d), 8.42 (2H, m), 8.24 (2H, d), 7.72 (4H, m), 7.29 (4H, m), 3.98 (4H, s), 2.57 (6H, s), 1.01 (4H, s).

### Synthesis of praseodymium, europium and gadolinium complexes

**PrL.** PrL was prepared as described previously for the LnL series.[38] Yield: 110 mg (0.153 mmol, 60.7 %). Elemental analysis, calcd for $[PrL(NO_3)_2](NO_3) \cdot 2H_2O$ (C24H24N9O11Pr); C 38.16, H 3.20, N 16.69: found: C 38.34, H 3.31, N 16.51; MS (FAB+); m/z, 657.1 [M – $NO_3^-$]$^+$ (calcd. 657.37).

**$PrL^{me}$.** $L^{me}$ (100 mg; 0.247 mmol) dissolved in 2 ml ethanol was mixed with an ethanol solution of $Pr(NO_3)_3 \cdot 6H_2O$ (111.8 mg, 0.257 mmol), and $PrL^{me}L$ was obtained as a white powder. Yield: 110 mg (0.150 mmol, 60.7%). Elemental analysis, calcd for $[PrL^{me}(NO_3)_2](NO_3) \cdot 2.5H_2O$ ($C_{25}H_{27}N_9O_{11.5}Pr$): C 38.57, H 3.50, N 16.19; found: C 38.62, H 3.44, N 16.26; MS (FAB$^+$); m/z, 671.08 [M – $NO_3^-$]$^+$ (calcd. 671.07).

**$PrL^{pr}$.** The complex was obtained as a white powder using the same protocol for $PrL^{me}$. Yield: 176 mg (0.240 mmol, 97.2%). MS (FAB$^+$); m/z, 671.09 [M – $NO_3^-$]$^+$ (calcd. 671.07).

**$PrL^{dmpr}$.** The complex was obtained as a white powder using the same method for $PrL^{me}$. Yield: 180 mg (0.236 mmol, 92.9%). Elemental analysis, calcd for $[PrL^{dmpr}(NO_3)_2](NO_3) \cdot 1.5H_2O$ ($C_{27}H_{29}N_9O_{10.5}Pr$): C 41.13, H 3.71, N 15.99; found: C 41.13, H 3.67, N 15.95; MS (FAB$^+$); m/z, 699.14 [M – $NO_3^-$]$^+$ (calcd. 699.11).

**PrLH, $PrL^{me}H$, $PrL^{pr}H$, and $PrL^{dmpr}H$.** Each Pr complex was obtained as a white powder by mixing of 100 mg of each ligand in ethanol with 111.8 mg of $Pr(NO_3)_3 \cdot 6H_2O$, then characterized.

*PrLH*. Yield 132 mg (0.179 mmol, 71.0%). MS (FAB$^+$); m/z, 661.1 [M – $NO_3^-$]$^+$ (calcd. 661.09).

*$PrL^{me}H$*. Yield 177 mg (0.239 mmol, 98.0%). MS (FAB$^+$); m/z, 675.13 [M – $NO_3^-$]$^+$ (calcd. 675.11).

*$PrL^{pr}H$*. Yield 122 mg (0.165 mmol, 67.6%). MS (FAB$^+$); m/z, 675.11 [M – $NO_3^-$]$^+$ (calcd. 675.11).

*$PrL^{dmpr}H$*. Yield 151 mg (0.197 mmol 86.4%). MS (FAB$^+$); m/z, 703.13 [M – $NO_3^-$]$^+$ (calcd. 703.14).

**Eu complexes.** The syntheses of EuL and EuLH were previously published.[41, 58] New complexes with Eu ions were obtained with the corresponding method of Pr above described.

*$EuL^{me}$*. Yield: 174 mg (0.234 mmol 94.7%). Elemental analysis, calcd for $[EuL^{me}(NO_3)_2](NO_3) \cdot 3H_2O$ ($C_{25}H_{28}N_9O_{12}Eu$): C 37.60, H 3.53, N 15.79; found: C 37.62, H 3.61, N 16.00; MS (ESI-TOF, acetonitrile); m/z, 683.29 [M – $NO_3^-$]$^+$ (calcd. 683.09).

*$EuL^{pr}$*. Yield: 82.1 mg (0.110 mmol 44.5%). Elemental analysis, calcd for $[EuL^{pr}(NO_3)_2](NO_3) \cdot 2H_2O$ ($C_{25}H_{26}N_9O_{11}Eu$); C 38.47, H 3.36, N 16.15; found; C 38.52, H 3.11, N 15.91; MS (ESI-TOF, acetonitrile); m/z, 683.29 [M – $NO_3^-$]$^+$ (calcd. 683.09).

*$EuL^{dmpr}$*. Yield: 74.1 mg (0.0959 mmol 37.8%). Elemental analysis, calcd for $[EuL^{dmpr}(NO_3)_2](NO_3) \cdot H_2O$ ($C_{27}H_{28}N_9O_{10}Eu$); C 41.02, H 3.57, N 15.95; found; C 40.91, H 3.53, N 16.23; MS (ESI-TOF, acetonitrile); m/z, 711.37 [M – $NO_3^-$]$^+$ (calcd. 711.12).

*EuL$^{me}$H*. Yield: 154.5mg (0.206 mmol 84.4%). MS (FAB$^+$); m/z, 687.11 [M – $NO_3^-$]$^+$ (calcd. 687.12).
*EuL$^{pr}$H*. Yield: 87.0 mg (0.116 mmol 47.5%). MS (FAB$^+$); m/z, 687.14 [M – $NO_3^-$]$^+$ (calcd. 687.12).
EuL$^{dmpr}$H. Yield: 65.0 mg (0.0817 mmol 35.8%). MS (FAB$^+$); m/z, 715.16 [M – $NO_3^-$]$^+$ (calcd. 715.15).

**Gd complexes.** Protocols for the synthesis of GdL and GdLH were previously published.[42, 55] New complexes with Gd ion were synthesized as described above for Pr complees.
*GdL$^{me}$*. Yield: 175 mg (0.233 mmol 94.3%). MS (ESI-TOF, acetonitrile); m/z, 688.18 [M – $NO_3^-$]$^+$ (calcd. 688.09).
*GdL$^{pr}$*. Yield: 87 mg (0.116 mmol 47.0%). MS (ESI-TOF, acetonitrile); m/z, 688.18 [M – $NO_3^-$]$^+$ (calcd. 688.09).
*GdL$^{dmpr}$*. Yield: 92 mg (0.118 mmol 46.5%). MS (ESI-TOF, acetonitrile); m/z, 716.22 [M – $NO_3^-$]$^+$ (calcd. 716.12).
*GdL$^{me}$H*. Yield: 116 mg (0.154 mmol 63.1%). MS (FAB$^+$); m/z, 692.15 [M – $NO_3^-$]$^+$ (calcd. 692.12).
*GdL$^{pr}$H*. Yield: 158 mg (0.210 mmol 64.8%). MS (FAB$^+$); m/z, 692.11 [M – $NO_3^-$]$^+$ (calcd. 692.12).
*GdL$^{dmpr}$H*. Yield: 47.6 mg (0.0608 mmol 26.7%).

**X-ray crystallography**

Single crystals of PrL, PrL$^{me}$, PrL$^{pr}$, Pr$^{dmpr}$, EuL$^{me}$, EuL$^{pr}$ and EuL$^{dmpr}$ were obtained from the recrystallization after replacing a counter anion from nitrato to hexafluorophosphate using $NH_4PF_6$.

X-ray structural data for PrL, PrL$^{me}$, PrL$^{pr}$, Pr$^{dmpr}$, EuL$^{me}$, EuL$^{pr}$ and EuL$^{dmpr}$ were collected on a Bruker Smart APEX-II CCD diffractometer equipped with graphite monochromated Mo Kα (1.54056 Å) radiation at 90 K. The data were collected to a maximum 2 h value of 55° and processed using the Bruker Apex2 (Bruker AXS Inc., 2004) software package. The structures were solved by the direct method using the program Sir2011,[60] and refined by full-matrix least-squares calculations using SHELXL2013.[61] All non-hydrogen atoms were refined anisotropically, and all hydrogen atoms were located at idealized positions. CCDC 1017809, 1043544, 1017810, 1043545, 1861235 and 1861236 contain the supplementary crystallographic data for PrL, PrL$^{me}$, PrL$^{pr}$, Pr$^{dmpr}$, EuL$^{pr}$ and EuL$^{dmpr}$, respectively. The data can be obtained from the Cambridge Crystallographic Data Centre via www.ccdc.cam.ac.jp/data_request/cif.

**Instrumentation and solvents**

Electronic absorption and luminescence spectra were recorded on a Shimadzu UV3600S and a Horiba Jobin-Ybon Fluorolog 3-22. NIR emission was detected by attaching a C1452-AU detector to the above apparatus. Luminescence quantum yields were measured using a C9920 Absolute PL Quantum Yield Measurement System (Hamamatsu Photonics K. K.).[62, 63] Luminescence lifetimes were obtained by Quantaurus tau (Hamamatsu Photonics K. K.). For the observation in solvents, ethanol as a glassy solvent and acetonitrile were used at 77 K and room temperature, respectively.

## Conclusions

The molecular photochemistry in organic compounds is mostly established the principle,[64] but it is not enough to design the high luminescent lanthanide complexes regarding the energy transfer still now. Here we identified a new class of Eu emission and Pr emission by using a series of helicate compounds. A series of Pr and Eu complexes with eight helicate ligands were examined and their luminescence behaviour were discussed. Single crystal X-ray analyses of these complexes showed that each complex formed a helicate structure with the hexadantate ligand. Eu complexes show typical red emissions, and the synthesized derivatives help to explain the intramolecular energy transfer efficiencies of this series of compounds. Judd-Ofelt analyses provided insights in to the radiative-/non radiative rate constants and the $\Omega_2$ values of these complexes. The luminescence intensity of Pr depends on molecular distortion and restraint of molecular vibration mode by the methylation. High-energy luminescence bands of Pr complexes were induced by reduction of the azomethine moiety on the ligand. In particular, we found the double excitation processes from both ligand and ff-absorption band for PrL will contribute to enhance ff-emissions, but normal antenna effect for PrL$^{pr}$.

## Conflicts of interest

There are no conflicts to declare.

## Acknowledgements.

The authors acknowledge Professor Jean-Marie Lehn, ISIS, Strasbourg University for fruitful discussions. We also thank Professor Yasunori Yamada, Saga University, for his advice to prepare racemic crystals. This work was partly supported by a Grants-in-Aid for Scientific Research on Innovative Areas “Soft Crystals; Area Number: 2903” (No. 17H06374; MH), MEXT Supported Program for the Strategic Research Foundation at Private Universities (2013-2017; MH), Network Joint Research Centre for Materials and Devices (2017-2019; MH). AI thanks the support of JST PRESTO “FRONTIR”.

## References

1. S. I. Weissman, *J. Chem. Phys.*, 1942, **10**, 214-217.
2. J.-C. G. Bünzli and C. Piguet, *Chem. Soc. Rev.*, 2005, **34**, 1048-1077.
3. E. G. Moore, A. P. S. Samuel and K. N. Raymond, *Acc. Chem. Res.*, 2009, **42**, 542-552.
4. L. Dai, W.-S. Lo, Y. Gu, Q. Xiong, K.-L. Wong, W.-M. Kwok, W.-T. Wong and G.-L. Law, *Chemical Science*, 2019, **10**, 4550-4559.
5. P. A. Tanner and C.-K. Duan, *Coord. Chem. Rev.*, 2010, **254**, 3026-3029.
6. G.-L. Law, K.-L. Wong, K.-K. Lau, S. Lap, P. A. Tanner, and W.-T. Wong, *J. Mater. Chem. C*, 2010, **20**, 4074-4079.
7. G.-L. Law, K.-L. Wong, X. Zhou, W.-T. Wong, and P. A. Tanner, *Inorg. Chem.*, 2005, **44**, 4142-4144.
8. J.-C. G. Bünzli, A.-S. Chauvin, H. K. Kim, E. Deiters and S. V. Eliseeva, *Coord. Chem. Rev.*, 2010, **254**, 2623-2633.
9. J.-C. G. Bünzli, *Coord. Chem. Rev.*, 2015, **293-294**, 19-47.

10. S. J. Butler and D. Parker, *Coord. Chem. Rev.*, 2013, **42**, 1652-1666.
11. B.-B. Du, Y.-X. Zhu, M. Pan, M.-Q. Yue, Y.-J. Hou, K. Wu, L.-Y. Zhang, L. Chen, S.-Y. Yin, Y.-N. Fana and C.-Y. Su, *Chem. Commun.*, 2015, **51**, 12533.
12. M. Pan, B.-B. Du, Y.-X. Zhu, M.-Q. Yue, Z.-W. Wei, and C.-Y. Su, *Chem. Eur. J.*, 2016, 22, 2440 – 2451.
13. S. V. Eliseeva, V. S. Liasotkyi, I. P. Golovach, P. G. Doga, V. P. Antonovich, S. Petoud and S. B. Meshkova, *Methods Appl. Fluoresc.*, 2017, **5**, 014002.
14. S. Ashokkumar, S. Ravi, V. Kathiravan and S. Velmurugan, *Spectrochimica Acta A*, 2017, **171**, 526.
15. K. Lorenz, E. Nogales, S. M. C. Miranda, N. Franco, B. Méndez, E. Alves, G. Tourbot and B. Daudin, *Acta Mater.*, 2013, **61**, 3278-3284.
16. H. Sun, D. Peng, X. Wang, M. Tang, Q. Zhang and X. Yao, *J. Appl. Phys.*, 2011, **110**, 016102.
17. W.-M. Liao, C.-J. Li, X. Wu, J.-H. Zhang, Z. Wang, H.-P. Wang, Y.-N. Fan, M. Pan and C.-Y. Su, *J. Mater. Chem. C*, 2018, **6**, 3254-3259.
18. G. Pawlicki and S. Lis, *Opt. Mater.*, 2011, **33**, 1544-1547.
19. R. V. Fox, R. D. Ball, P. d. B. Harrington, H. W. Rollins, J. J. Jolley and C. M. Wai, *J. Supercrit. Fluids*, 2004, **31**, 273-286.
20. M. Irfanullah and K. Iftikhar, *J. Fluorescence*, 2011, **21**, 673-686.
21. V. M. Pereira, A. L. Costa, J. Feldl, T. M. R. Maria, J. S. Seixas de Melo, P. Martín-Ramos, J. Martín-Gil and M. Ramos Silva, *Spectrochimica Acta A*, 2017, **172**, 25-33.
22. M. A. Zaitoun, A. K. El-Qisairi, K. A. Momani, H. A. Qaseer and Q. M. Jaradat, *Spectrochimica Acta A*, 2015, **136**, 1745-1750.
23. E. A. Mikhalyova, A. V. Yakovenko, M. Zeller, K. S. Gavrilenko, S. E. Lofland, A. W. Addison and V. V. Pavlishchuk, *Inorg. Chim. Acta*, 2014, **414**, 97-104.
24. P. R. Matthes, J. Nitsch, A. Kuzmanoski, C. Feldmann, A. Steffen, T. B. Marder and K. Müller-Buschbaum, *Chem. Eur. J.*, 2013, **19**, 17369-17378.
25. L. Wang, W. Gu, X.-J. Deng, L.-F. Zeng, S.-Y. Liao, M. Zhang, L.-Y. Yang and X. Liu, *Aust. J. Chem.*, 2011, **64**, 1373-1382.
26. X. S. Tai and L. T. Wang, *Adv. Mat. Res.*, 2011, **219-220**, 565-568.
27. S. B. Meshkova, Z. M. Topilova, V. S. Matiichuk, N. T. Pokhodylo, I. P. Kovalevskaya, I. M. Rakipov and P. G. Doga, *Russian. J. Coord. Chem*, 2011, **37**, 309-315.
28. R. Feng, F.-L. Jiang, M.-Y. Wu, L. Chen, C.-F. Yan and M.-C. Hong, *Cryst. Growth Des.*, 2010, **10**, 2306-2313.
29. Z. A. Siddiqi, M. Shahid, M. Khalid, S. Noor and S. Kumar, *Spectrochimica Acta A*, 2009, **74**, 391-397.
30. M. D. Regulacio, M. H. Pablico, J. A. Vasquez, P. N. Myers, S. Gentry, M. Prushan, S.-W. Tam-Chang and S. L. Stoll, *Inorg. Chem.*, 2008, **47**, 1512-1523.
31. S. Quici, M. Cavazzini, G. Marzanni, G. Accorsi, N. Armaroli, B. Ventura and F. Barigelletti, *Inorg. Chem.*, 2005, **44**, 529-537.
32. N. Yoshida, A. Matsumoto and J. Shiokawa, *Bull. Chem. Soc. Jpn.*, 1974, **47**, 648-651.
33. G. M. Davies, H. Adams, S. J. A. Pope, S. Faulkner and M. D. Ward, *Photochem. Photobiol. Sci.*, 2005, **4**, 829-834.
34. G. M. Davies, R. J. Aarons, G. R. Motson, J. C. Jeffery, H. Adams, S. Faulkner and M. D. Ward, *Dalton Trans.*, 2004, 1136-1144.
35. N. K. Al-Rasbi, S. Derossi, D. Sykes, S. Faulkner and M. D. Ward, *Polyhedron*, 2009, **28**, 227-232.
36. L. Aboshyan-Sorgho, M. Cantuel, S. Petoud, A. Hauser and C. Piguet, *Coord. Chem. Rev.*, 2012, **256**, 1644-1663.
37. S. B. Meshkova, A. V. Kiriyak and Z. M. Topilova, *J. Appl. Spectrosc.*, 2006, **73**, 834-840.
38. S. B. Meshkova, A. V. Kiriyak, Z. M. Topilova and V. P. Antonovich, *J. Anal. Chem.*, 2007, **62**, 362-365.
39. M. Hasegawa, A. Ishii and S. Kishi, *J. Photochem. Photobiol. A: Chem.*, 2006, **178**, 220-224.
40. E. C. Constable, R. Chotalia and D. A. Tocher, *J. Chem. Soc., Chem. Commun.*, 1992, 771-773.
41. C. Piguet and J.-C. G. Bünzli, in *Handbook on the Physics and Chemistry of Rare Earths*, eds. K. A. Gschneidner, J.-C. G. Bünzli and V. K. Pecharski, Elsevier, 2010, vol. 40, pp. 301-553.
42. M. Hasegawa, H. Ohtsu, D. Kodama, T. Kasai, S. Sakurai, A. Ishii and K. Suzuki, *New J. Chem.*, 2014, **38**, 1225-1234.
43. H. Wada, S. Ooka, D. Iwasawa, M. Hasegawa and T. Kajiwara, *Magnetochemistry*, 2016, **2**, 43.
44. M. Hatanaka, A. Osawa, T. Wakabayashi, K. Morokuma and M. Hasegawa, *Phys. Chem. Chem. Phys.*, 2018, **20**, 3328-3333.
45. Y. Hasegawa, A. Ishii, Y. Inazuka, N. Yajima, S. Kawaguchi, K. Sugimoto and M. Hasegawa, *Molecules*, 2018, **23**, 55.
46. M. Hasegawa, D. Iwasawa, T. Kawaguchi, H. Koike, A. Saso, S. Ogata, A. Ishii, H. Ohmagari, M. Iwamura and K. Nozaki, *ChemPlusChem*, 2020, **85**, 294-300.
47. G. H. Dieke and H. M. Crosswhite, *Appl. Opt.*, 1963, **2**, 675-686.
48. W. T. Carnall, P. R. Fields and R. Sarup, *J. Chem. Phys.*, 1969, **51**, 2587-2591.
49. W. T. Carnall, P. R. Fields and K. Rajnak, *J. Chem. Phys.*, 1968, **49**, 4424-4442.
50. M. D. Ward, *Coord. Chem. Rev.*, 2010, **254**, 2634-2642.
51. D. L. Dexter, *J. Chem. Phys.*, 1953, **21**, 836-850.
52. B. R. Judd, *Phys. Rev.*, 1962, **127**, 750-761.
53. G. S. Ofelt, *J. Chem. Phys.*, 1962, **37**, 511-520.
54. K. Binnemans, *Coord. Chem. Rev.*, 2015, **295**, 1-45.
55. S. Wada, Y. Kitagawa, T. Nakanishi, M. Gon, K. Tanaka, K. Fushimi, Y. Chujo and Y. Hasegawa, *Sci. Rep.*, 2018, **8**, 16395.
56. S. Ogata, N. Goto, S. Sakurai, A. Ishii, M. Hatanaka, K. Yoshihara, R. Tanabe, K. Kayano, R. Magaribuchi, K. Goto and M. Hasegawa, *Dalton Trans.*, 2018, **47**, 7135-7143.
57. S. Ogata, H. Komiya, N. Goto, R. Tanabe, K. Sugimoto, S. Kawaguchi, K. Goto, M. Hatanaka, A. Ishii and M. Hasegawa, *Chem. Lett.*, 2019, **48**, 593-596.
58. C. Y. Chow, S. V. Eliseeva, E. R. Trivedi, T. N. Nguyen, J. W. Kampf, S. Petoud and V. L. Pecoraro, *J. Am. Chem. Soc.*, 2016, **138**, 5100-5109.
59. S. Ogata, T. Shimizu, T. Ishibashi, Y. Ishiyone, M. Hanami, M. Ito, A. Ishii, S. Kawaguchi, K. Sugimoto and M. Hasegawa, *New J. Chem.*, 2017, **41**, 6385-6394.
60. M. C. Burla, R. Caliandro, M. Camalli, B. Carrozzini, G. L. Cascarano, L. De Caro, C. Giacovazzo, G. Polidori and R. Spagna, *J. Appl. Crystalloagr.*, 2005, **38**, 381-388.
61. T. Gruene, H. W. Hahn, A. V. Luebben, F. Meilleur and G. M. Sheldrick, *J. Appl. Crystallogr.*, 2014, **47**, 462-466.
62. R. Katoh, K. Suzuki, A. Furube, M. Kotani and K. Tokumaru, *J. Phys. Chem. C*, 2009, **113**, 2961-2965.

63. K. Suzuki, A. Kobayashi, S. Kaneko, K. Takehira, T. Yoshihara, H. Ishida, Y. Shiina, S. Oishi and S. Tobita, *Phys. Chem. Chem. Phys.*, 2009, **11**, 9850-9860.

64. N. J. Turro, V. Ramamurthy and J. C. Scaiano, *Modern Molecular Photochemistry of Organic Molecules*, 2012.

Table of Contents